IAC-07- C4.4.07

Characterization of a T6 Based Hollow Cathode Thruster

Presented at the 58th International Astronautical Federation Congress, Hyderabad, India
September 24th - 28th, 2007

Angelo N. Grubisic* and Stephen B. Gabriel,*
Astronautics Research Group, University of Southampton, Southampton, SO17 1BJ, United Kingdom

David G. Fearn*
Electric Propulsion Solutions, Fleet, Hants, GU14 0LX, United Kingdom

Abstract: This paper characterizes thrust performance of a variant of the T6 hollow cathode modified for improved operational characteristics. The device displays promising performance and highlights the potential for application as a microthruster. The T6 cathode is able to produce specific impulse of over 1050s with xenon and argon; however the dominant acceleration mechanism at low flow rates is shown to be almost entirely electromagnetic effectively constituting a low power, magneto-plasma-dynamic thruster. The modified cathode also displayed very low discharge voltages ~12V and stable operation while carrying currents as high as 30-Amps on flow rates of less than 0.1mgs^{-1} down to 0.04mgs^{-1} with xenon. This investigation also highlights the importance of electrode geometry in hollow cathode thruster design and indeed in all other applications of hollow cathode where flow rates should be minimized.

Nomenclature

α	=	Degree of ionization
A	=	Area, m^2
amu	=	Atomic mass unit
C_p	=	Specific heat capacity, kJ/kg.K
d	=	Diameter, m
ε_i	=	Ionization potential, eV
e	=	Electron charge, C
E	=	Electric field, V/m
f	=	View factor
I	=	Current, A
J	=	Current density, A/m^2
k	=	Boltzman's constant, 1.381×10^{-23} J/K
L	=	Characteristic length, m
m	=	Particle mass, kg
$\dot{m}$	=	Mass flow rate, kg/s
n	=	Particle density, m^{-3}
p	=	Internal cathode pressure, N/m^2
P	=	Power, W
q_r	=	Radiative heat flux, W
r	=	Radius, m
R	=	Resistance, Ohms
T	=	Temperature, K
μ	=	Magnetic permeability
V	=	Potential, V
η	=	Plasma resistivity, Ohm/m
λ_d	=	Debye length, m
$ln\Lambda$	=	Coulomb logarithm
V_p	=	Plasma potential, V
v	=	Velocity, m/s
σ	=	Electrical conductivity, Ohms/m
y	=	Ratio of specific heats (5/3 for xenon)

Subscripts

A	=	Anode
n	=	Neutrals
c	=	Cathode
D	=	Discharge current
d	=	Debye
ds1,2	=	Double sheath at orifice entrance and exit
e	=	Electrons
eq	=	Equivalent
ex	=	Exit
eff	=	Effective
em	=	Emitter
f	=	Fall

i	=	Ions
k	=	Keeper
oh	=	Ohmic
o	=	Orifice
s	=	Static

INTRODUCTION

THIS paper provides characterization of a T6 hollow cathode in the role of a standalone microthrusters. The T6 cathode is a mature device developed extensively over the last 35-years for application on the UK-25, and T6 gridded ion thrusters [1 2 3 4 5 6] and as an electron source for various ion beam neutralization applications.[7] Previous testing at the University of Southampton on the T6 hollow cathode has shown that at least a basic thruster can be formed, generating moderate specific impulse (<300s with xenon) at thrust levels <2 milli-Newtons, however no attempt was made to optimize the device for improved performance.[8 9 10]

Hollow cathodes may represent an attractive propulsion device for a number of reasons besides performance. Spacecraft which operate primary electrostatic or electromagnetic propulsion systems such as gridded ion thrusters and Hall thrusters are typically required to carry a secondary chemical system for reaction/momentum control or to compensate for thrust misalignment.[11 12 13 14] These secondary systems constitute a large fraction of the overall propulsion system mass while they are only required to produce a small fraction of the total impulse. These systems also bring substantial cost increases in manufacture, assembly, integration, test operations, and launch preparation primarily due to hazardous propellants.[15] A simpler solution would be to use a moderate performance secondary system able to operate from a common inert propellant with the primary system; however the high molecular mass of xenon limits the performance of cold gas thrusters and resistojets to between 15-48s specific impulse. [16 17] If hollow cathodes can be optimized as thrusters and show better performance, they may be well suited to this purpose. Concurrent design studies as part of this work have highlighted the possibility of producing an all-electric lunar transfer orbiter utilizing the T5 gridded ion thruster and 8 hollow cathode AOCS thrusters at less than 150kg wet mass.[18] A similar NEO rendezvous mission study utilizing 3 microsatellites with T5 gridded ion thrusters and T6 hollow cathode thrusters also generated relatively low-cost spacecraft (50 M€ for the first and 30 M€ for subsequent spacecraft) with a wet mass of less than 120kg each. [19]

The relatively low operating power of hollow cathodes such may also present a microthruster suitable for smaller satellites (<150kg). Guidelines issued by the Inter-Agency Space Debris Coordination Committee (IADC) recommend that spacecraft in low earth orbit have the ability to deorbit within 25-years. This increases the mission delta-V by some 100-500% for typical earth observation missions.[20] As demands on small spacecraft also continue to grow for missions such as formation-flying, inspection and rendezvous, requiring drag compensation, constellation phasing and proximity maneuvering,[21] conventional robust microsatellite propulsion systems such as cold gas thrusters and resistojets are deficient in performance. Microsatellite platforms however lack the resources to support advanced enabling technologies such as micro-ion engines and Hall thrusters. The diffuse arc in the T6 hollow cathode in particular permits operation at convenient discharge voltages (10-25V) for satellites with limited power electronics, especially when compared to other electrothermal, electrostatic or electromagnetic thrusters. [22] Furthermore a hollow cathode microthrusters system would able to draw from existing inert propellant storage and feed architectures for conventional cold gas/resistojet systems which find considerable use on small satellites due to their simplicity and low cost nature. This makes their addition a reasonably simple process. The inert propellant also bares no contamination risk to sensitive spacecraft equipment when compared with other thrusters in the milli-Newton thrust range such as PPT's (Pulsed Plasma Thrusters), colloid and FEEP (Field Emission Electric Propulsion) thrusters. [23] Many hollow cathodes have significant space heritage and would therefore require minimal requalification. Hollow cathode thrusters may therefore be a fitting compromise if their performance is sufficient.

Cathode Operation and Description

The T6 Hollow Cathode used in this experiment is derived from neutralizer of the ROS-2000 HET (Hall Effect Thruster) (developed by QinetiQ for Astrium under contract to ESA) and is shown in Figure 1. The cathode is rated to a maximum of 30-Amps with extended operation up to 50-Amps with flow rates ranging from 0.1-3mg/s, typically operating at a few hundred watts. The cathode contains a tungsten dispenser, 2mm i.d. x 5mm o.d. x 10mm, impregnated with a mixture of barium-oxide, calcium oxide and aluminates (BaO: CaO: Al_2O_3), which lowers the insert's work function for thermionic emission, and maintains a working temperature of approximately 1000°C. At maximum rated current capacity, the T6 dispenser emits with a current density of at least at least 1500 $A.cm^{-2}$.

Figure 1 T6 ROS-2000 HET Neutralizers

The cathode is constructed from a solid tantalum piece with a 1mm axial orifice through a 2mm thick faceplate with a 45° chamfer at the exit to a depth of 1mm leaving an orifice of 1mm length. In this case the T6 anode and support housing has been specially designed to maximize available anode-plasma contact area on the basis that this parameter has a strong influence on the minimum attainable flow rate and in reducing the discharge voltage (discussed more fully in the next section). The T6 cathode is mounted to a ceramic insulator which also connects to the anode housing. A 25mm diameter 30° conical diverging nozzle constructed from graphite with a 4mm orifice at the upstream end is mounted 0.5mm in front of the cathode and axially aligned. All flanges are sealed with grafoil gaskets. The T6 thruster is shown in Figure 2.

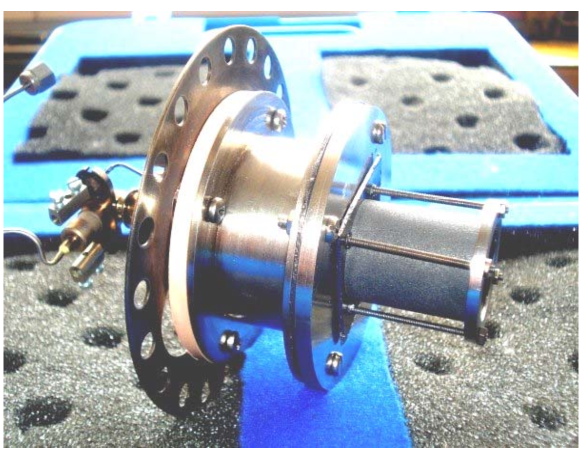

Figure 2 T6 hollow cathode thruster variant with modified anode and housing

In typical hollow cathodes a keeper electrode usually draws approximately 1-Amp of current, however in this study the cathode is operated in an open-diode configuration with the full discharge current being drawn to the keeper, which is now termed the anode. Open-diode configuration is more representative of a standalone microthruster configuration with no need for a coupled discharge.

<u>Ignition and Operation</u>

An internal cutaway of a T5 cathode is shown in Figure 3 which is at least functionally comparable to the T6. A tungsten heater is used to raise the temperature of the emitter (>1000°C) sufficient for initial thermionic emission. A trigger voltage applied to an external electrode is typically used to initiate the discharge (15-200V). The orifice plate increases the internal pressure and generates sufficiently dense plasma within the internal volume to promote ion recombination at the emitter surface. Self-heating is then maintained by the acceleration of ions through the sheath (region between the cathode and plasma column), which recombine on internal surfaces to form neutrals. Confining the plasma column within the hollow cavity of the cathode permits operation at low cathode fall voltages while allowing high currents to be carried.

The plasma column induces sheath-enhanced emission at the emitter surface due to the intense field ($\sim 10^7$V/m) between the plasma column and cathode potentials at a distance on the order of the Debye length. These impregnate constituents undergo thermo-chemical reactions and liberate free Ba/BaO/CaO, which are adsorbed from the emitting surface during heating and operation. These components introduce a dipole and decrease the elecronegativity barrier of the emitting surface, corresponding to a decrease in work function for thermionic emission.[24] Emitter life is generally based on the ability of the emitter to liberate free barium, where the rate of desorption is considered temperature dependant and a function of the emitted current density.

Thermionically emitted electrons are accelerated through the sheath potential and considered as a mono-energetic beam. The plasma potential within the emitter volume generally remains 8-10V above the cathode potential (however lower values are recorded in large orifice cathodes) consistent with the energy required for the excitation of meta-stable states of xenon ($3P_0$ ~ 9.45eV, $3P_2$ ~8.32eV). Ion

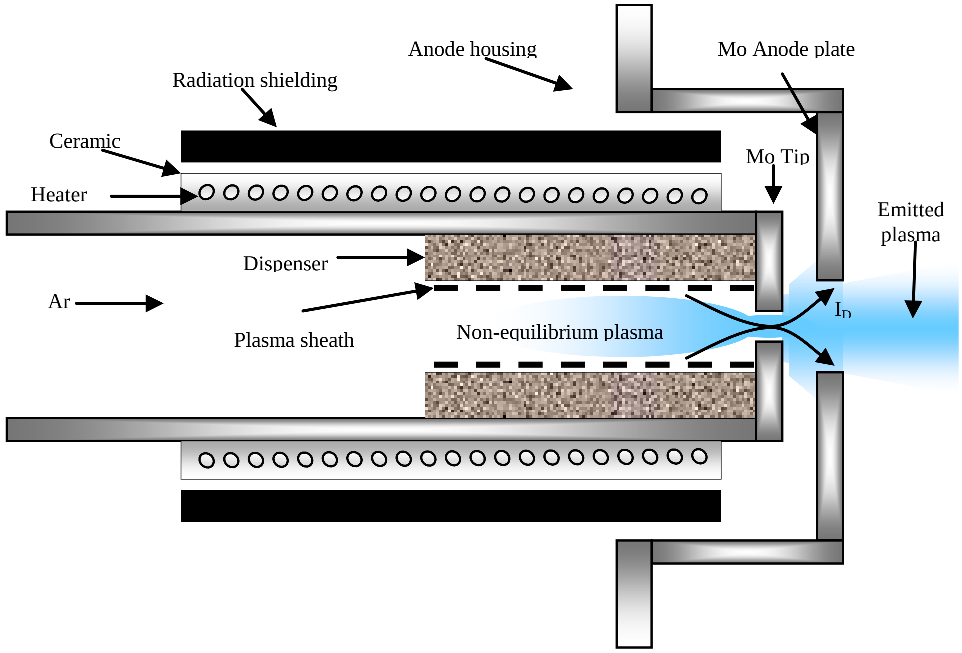

Figure 3 Internal schematic of a T5 cathode

production is generally assumed to be achieved by multi-step processes firstly by electron impact of primary electrons from the atomic ground state[25] within the emitter volume, and then by lower energy thermalized electrons (2-4eV) within the orifice which then contribute significantly to the ionization process. The total process thus requires transfer of at least the ionization energy (12.13eV for xenon). The discharge current is drawn through the orifice toward the anode. Processes within the orifice dominate performance. The operating regime acts to maintain emitter temperatures for thermionic emission by balancing power deposition to the cathode with cooling by particle efflux and heat transfer to the surroundings.

Energy input to the plasma can be attributed to the energy of thermionically emitted electrons accelerated through the cathode fall and through Ohmic (collisional) heating within the orifice channel. While direct measurements have not fully characterized the processes following ignition, it is considered that xenon plasma initially forms between the orifice plate and the anode. This plasma extends into the hollow core of the cathode insert. Coupling of the electric field into this region drives the ionization electrons that ultimately provide the breakdown of the main discharge. Since Ohmic heating of the plasma volume within the emitter is small compared to the orifice due to relative number densities in the respective volumes, orifice geometry drives resistive dissipation and energy equipartition to the plasma. This may have a strong influence on an electrothermal thruster's performance.

Spot and Plume Modes

Spot and plume-modes are the two major discharge regimes considered in orificed hollow cathode design, especially important when operating off a small satellite bus at low powers. If the flux of ions into the cathode-anode gap is sufficient, the anode will passively collect the discharge current from the plasma. This type of operation is referred to as spot mode. If the ion flux to the cathode-keeper gap is not sufficient for the anode to passively collect the electron current, an additional voltage drop forms between the plasma and anode to facilitate ionization so that electrons can traverse the gap within the quazi-neutral plasma. This occurs as the mass flow rate or discharge current is decreased beyond a critical point, and is termed plume mode. Since in plume mode the ions created in the gap have some fraction of the cathode fall to accelerate them toward the cathode orifice plate, it exhibits ion sputtering[26] and discharge instabilities, which limit lifetime[27] and give high coupling voltages. As in cathode development for ion engines, consideration must be given to maintain reasonable discharge voltages and operating temperatures for adequate lifetime. This is normally limited by impregnate depletion in Kaufman type ion engines and ion sputtering in ring-cusp chamber designs. Application as an electrothermal thruster may demand high current densities within the orifice to maximize Ohmic heating therefore the maximum tolerable tip temperature for adequate thruster life will dictate the limiting current density and maximum acceptable power deposition into the orifice. Operation at orifice plate temperatures below 1300°C has typically been used in development of low power low flow 3.2mm cathodes consistent with practices proven to enable lifetimes greater than 10,000 hr.[28]

Energy Balance

At the hollow cathode surface the dominant energy gain processes are thermal energy input by ion bombardment and hot plasma electrons with energies sufficient to exceed the cathode fall voltage, while energy is lost by convective cooling, thermionic emission and radiative flux. This power balance is represented by:

$$\int J_{th}\left(\phi_{eff} + \frac{5kT_c}{2e}\right) dA_e =$$

$$\int J_i\left(\varepsilon_i + V_f - \phi_{eff}\right) dA_e + \int J_e\left(\phi_{eff} + \frac{5kT_e}{2e}\right) dA_e - fq_r \tag{1}$$

With a view factor from the emitter to the cathode body:

$$f = \frac{A_e}{A_s} \tag{2}$$

The power delivered by the ions consists of the kinetic energy of the impact and the energy released when the ion recombines. The energy of the thermionic electrons can be approximated as a mono-energetic beam since the energy gained by acceleration through the sheath is much greater than the thermal energy, and assumes a collisionless sheath. In this analysis it is assumed that energy deposited into the cathode surfaces other than the emitter does not return to the plasma except as radiation and heating of cold neutral atoms.

Plasma Power Balance

Since the emitter temperature profile is not constant along the length of the cathode[29, 30], integrals allow for the resulting variation in current density from the emitter. Electron emission provides energy to the plasma in the form of electrons accelerated by the cathode fall. This energy is utilized to ionize and excite the gas, and heat the plasma electrons. Energy is also added to the plasma by Ohmic heating of the resistive plasma within the orifice. Energy is lost by particles flowing out of the cathode, given by:

$$\int J_{th}\left(V_p + \frac{5kT_e}{2e}\right) dA_{em} + \int \frac{J_D^{\ 2}}{\sigma} dV =$$
$$\int J_i\left(\varepsilon_i + \frac{5kT_i}{2e}\right) dA_s + \int J_e\left(\frac{5kT_e}{2e}\right) dA_s$$
$$+\left(I_D + \alpha I_{eq}\right)\left(\frac{5kT_e}{2e}\right) + \frac{I_{eq}}{\alpha}\left(\frac{5kT_e}{2e}\right) + q_r \tag{3}$$

Where equivalent flow rate is defined by:

$$I_{eq} = \frac{e\dot{m}}{m_i} \tag{4}$$

If the configuration of the thruster allows for the condition of fully ionized plasma at the orifice exit with a high degree of gas utilization, then the energy balance can be expressed as:

$$I_{th}\left(V_p + \frac{5kT_e}{2e}\right) + \int \frac{I_D^{\ 2}}{\sigma} dV_{oh} =$$
$$I_i\left(\varepsilon_i + \frac{5kT_i}{2e}\right) + I_e\left(\frac{5kT_e}{2e}\right)$$
$$+\left(I_D + I_{eq}\right)\left(\frac{5kT_e}{2e}\right) + I_{eq}\left(\frac{5kT_i}{2e}\right) + q_r \tag{5}$$

This assumes Ohmic heating of the plasma volume within the emitter is small compared to the orifice due to relative number densities in the respective volumes.

Discharge Parameters

The total discharge current is based on the contributions of all particle fluxes at the cathode surface for preservation of current continuity and is expressed as:

$$I_D = I_{th} + I_i - I_e \quad (6)$$

The total discharge voltage can be expressed as:

$$V_d = V_p + \Delta V_{ds1} + \Delta V_{oh} + \Delta V_{ds2} \quad (7)$$

This is the sum of the cathode fall voltage, the Ohmic drop across the orifice and the double sheaths at the entrance and exit of the orifice.

Energy Conservation

At the insert surface, the energy loss due to convected thermionic electrons is balanced primarily by ion bombardment. If energy input due to plasma electrons overcoming the fall voltage is neglected (since the fall voltage is much greater than most of the electron energies for a Maxwellian distribution) the energy balance can be expressed as:

$$\int J_{th}\left(\phi_{eff} + \frac{5kT_c}{2e}\right)dA_e = \int J_i\left(\varepsilon_i + V_f - \phi_{eff}\right)dA_e \quad (8)$$

The working temperature of a given emitter is therefore a product of the fall voltage, particle densities and emitter geometry for sustained thermionic emission.

Plume Mode Transition

To ensure the cathode consistently operates in spot mode the thermal flux of electrons to the anode must be at least be equal to the discharge current. An empirical transition to spot mode criterion[31] has been described by Kaufman, which accurately predicted the transition flow rate. Katz has numerically determined this transition on the basis of the contact area of the anode with the downstream plasma. The necessary surface area of anode is calculated by the thermal flux of electrons to the surface. The ratio of discharge current to passively collected electron current at the anode surface is given by:

$$\frac{I_D}{I_A} = \frac{I_D}{I_i}\left(\frac{r_{AK}^2}{A_A}\right)4\pi^{3/2}\sqrt{\frac{m_e T_i}{m_i T_e}} \quad (9)$$

where the plasma density is determined from the proportion of the ion output from the orifice, which is in contact with the anode surface.

Dimensions of the anode aperture in the T6 anode design were selected to allow for at least 50-Amps of discharge current to be collected for testing purposes even with gas utilization as low as 10% since the high utilization assumption may not be reflected in experiment. A thermal model of the T6 cathode thruster assembly is shown in Figure 5. This was used in the thermal design and hence graphite was selected for the anode nozzle due to the heat deposited primarily by convective heat transfer from the dispenser surface by electrons during operation.

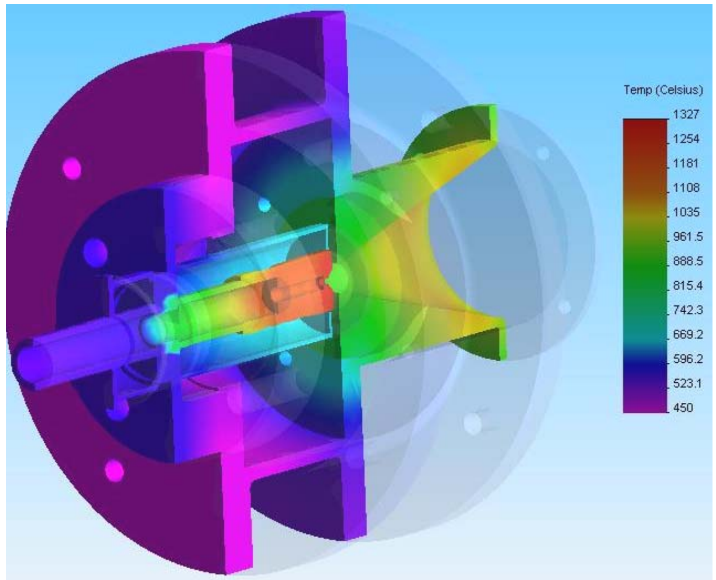

Figure 4 T6 Hollow cathode thruster assembly thermal model operating at 30A with argon on 0.05mgs^{-1}

THRUST PRODUCTION

Plasma models suggest that cathodes are capable of generating peak heavy particle temperatures greater than 6,000K with wall temperature not exceeding 1,500K.[32] Laser Induced Fluorescence (LIF) has identified neutral temperatures in cathode-keeper gaps are between 1800-4000K, well above cathode wall temperature.[33] Experiment has also suggested heavy particle temperatures between 3200-6000K necessary to explain elevated backpressures within conventional cathodes.[34] Assuming the plasma and remaining neutrals undergo some degree of adiabatic expansion it is reasonable to assume some level of thermal energy conversion to directed kinetic energy of the flow which is dependant on the plasma heating modes. The main mechanism of plasma heating is known to be Ohmic heating by plasma electrons within the cathode orifice with collisional heat transfer to the heavy particles.[35] A thermal thrust mechanism with significant arc heating within the cathode would be possible while low wall temperatures are maintained (<1700K) given the low plasma densities contacting the orifice (~10^{20}/m ^{3}) [36] The electron temperature within the orifice is typically 11,600-23,200K (1-2eV), depending on the degree of Ohmic heating. The performance of any electrothermal device can be approximated by means of a rudimentary one-dimensional energy argument that limits the exhaust speed of the flow from a fully expanded nozzle to:

$$v_{ex} \leq \sqrt{C_p T_{prop}} \tag{10}$$

When considering thermalization of the propellant to produce thrust with xenon, krypton or argon, the theoretical limit to specific impulse (assuming full conversion of thermal to directed kinetic energy) is shown in Figure 5.

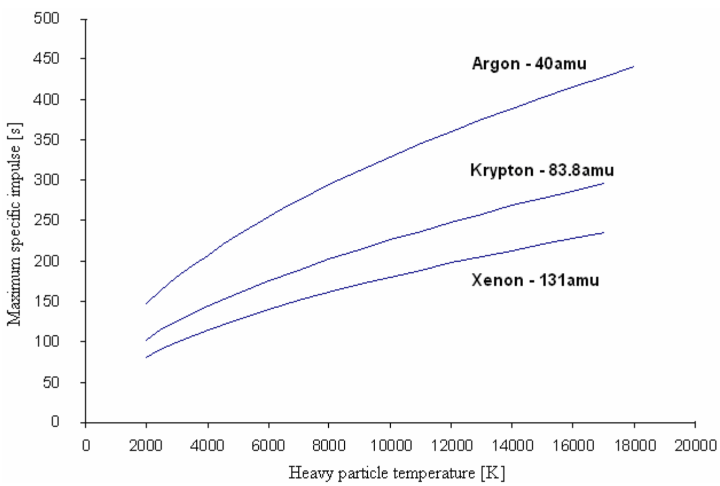

Figure 5 Limiting specific impulse for thermalized propellants based on full energy conversion

Accounting for the specific impulse found from the T6 even in early testing requires heavy particle temperatures too high to be described by a thermal thrust mechanism alone. The T6 may therefore experience a degree of electromagnetic acceleration of the charged particles by pinch forces in the plasma, which is reasonable at 25 Amps. The T5 cathode however operates at much lower currents and therefore is expected to operate in an almost purely electrothermal mode. Thrust production by magneto-plasma-dynamic forces, pressure and momentum thrust at the orifice exit can be estimated by assuming a blowing force acts on the plasma and by the various particle pressures at the orifice exit.

Assuming that a cathode is able to operate at very low flow rates where the degree of pressure contribution may be assumed negligible, it can be shown that MPD acceleration forces become increasingly dominant. A stream wise acceleration is provided by the crossing of the radial arc current with the self generated azimuthal magnetic field through the cathode orifice, an essentially scalar crossed-field interaction given by:

$$F_z = \frac{\mu J^2}{4\pi}\left(\ln\frac{r_a}{r_c} + \frac{1}{4}\right) \tag{15}$$

Assuming the current density through the orifice is uniform, a virtual cathode radius can be set to the orifice diameter with the appropriate coefficient. The theoretical specific impulse arising from the blowing component when operating the given T6 setup described earlier at 30, 20 and 10 Amps for any given propellant can be estimated. Theoretical specific impulse arising from the blowing force at any propellant mass flow rate is shown in Figure 7.

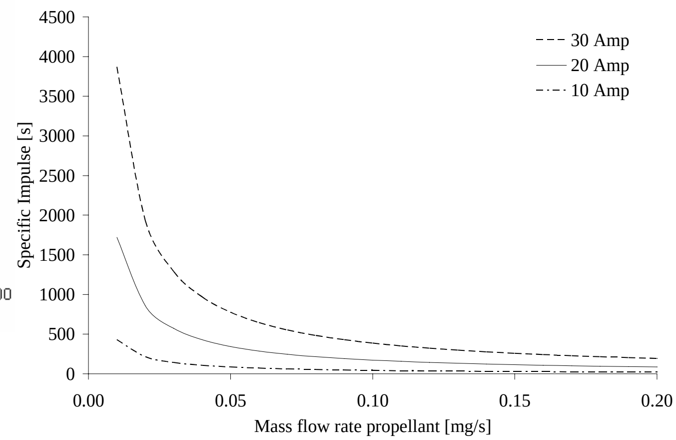

Figure 6 Theoretical specific impulse as a result of blowing force from the given T6 setup

One would be inclined to think that the total blowing force would be much smaller since there also exists a counterproductive blowing force at the orifice entrance (from the movement of the electron current from the insert towards the constricted orifice) which is only loosely dependant on geometry and must therefore be similar to the thrusting force. However the counter blowing force merely causes an artificial backpressure buildup within the internal cavity of the cathode which reaches equilibrium with the counter-blowing force to maintain a constant mass flow rate. This internal blowing force, while being important in establishing the internal operating parameters of the cathode, especially at low mass flow rate, can be neglected in the thrust production process.

Assuming two cathodes of equal orifice and anode diameters to the T5 and modified T6 cathodes (0.25mm, 3mm and 1mm, 25mm respectively) theoretical thrusts for blowing force are shown in Figure 7. It should be noted that the discharge currents considered here are well in excess of the rated operating currents for the T5 cathode however it does show the significance of geometry in production of the blowing force.

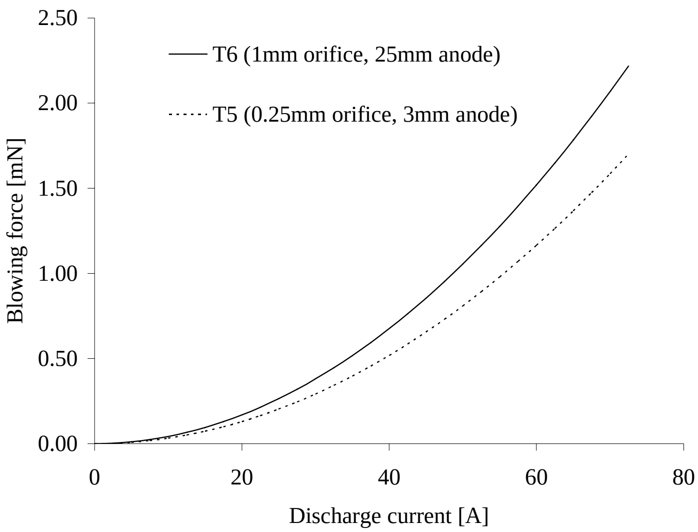

Figure 7 Blowing force with discharge current for two configurations of hollow cathode

EXPERIMENTAL SETUP

Vacuum Rig

The vacuum rig used in this experiment is described in [37] previously used for hollow cathode characterization within the UK-25 ion engine. The rig consists of a 500mm diameter by 500mm long chamber with ISO and CF flanges. A cylindrical water cooled copper shroud fitted around the inside of the vacuum chamber wall is used to dissipate heat load. Pumping is achieved with a water-cooled turbo molecular pump (Pfeiffer Balzers TPH 520KTG, 500l/s) controlled by a TCP 380 power supply (with a TCS303 pump control unit) and backed by a rotary vane pump (Edwards EH500A H/C 80 CMH), achieving an ultimate vacuum of 10^{-8} mbar. This level of vacuum ensures the partial pressure of oxygen in the system is low enough to prevent poisoning of the chemically sensitive thermionic emitter. Propulsion grade argon (99.997% pure) is passed through high and low capacity oxygen traps via an Edwards FCV10K extra fine control needle valve.

Power Supplies

In operation of the T6 cathode as a stand-alone thruster, the number of power supplies is reduced to three. It is also worth noting that since the cathode is in effect self-neutralizing, there is no need to electrically float the thruster system to a high positive potential, removing the requirement for electrical isolation of the thruster mounts and propellant feed lines. The electrical wiring system inside the chamber is also designed to minimize the influence of any MHD effects on the plasma both within the cathode and on the externally emitted plasma which may influence the thrust vector. The power supply system is shown schematically in Figure 8.

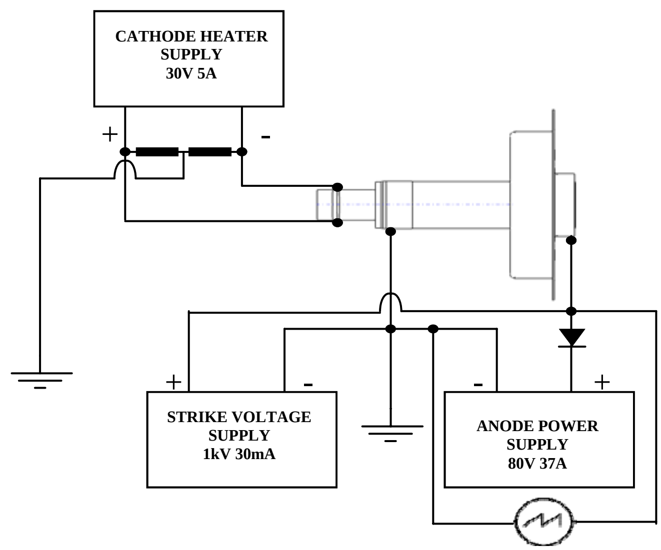

Figure 8 Electrical setup schematic

The cathode heater supply (Powerbox Lab605) provides the 2.2A required to heat the cathode to ignition temperatures (>1000˚C) prior to discharge ignition. The heater supply is operated in constant current mode with a common ground to the cathode potential to minimize the voltage difference between the heater wire and cathode body, reducing the risk of heater insulation breakdown. The discharge power supply consists of a high voltage (1kV, 30mA) strike supply and a low voltage (80V, 37A) steady state supply protected by diodes.

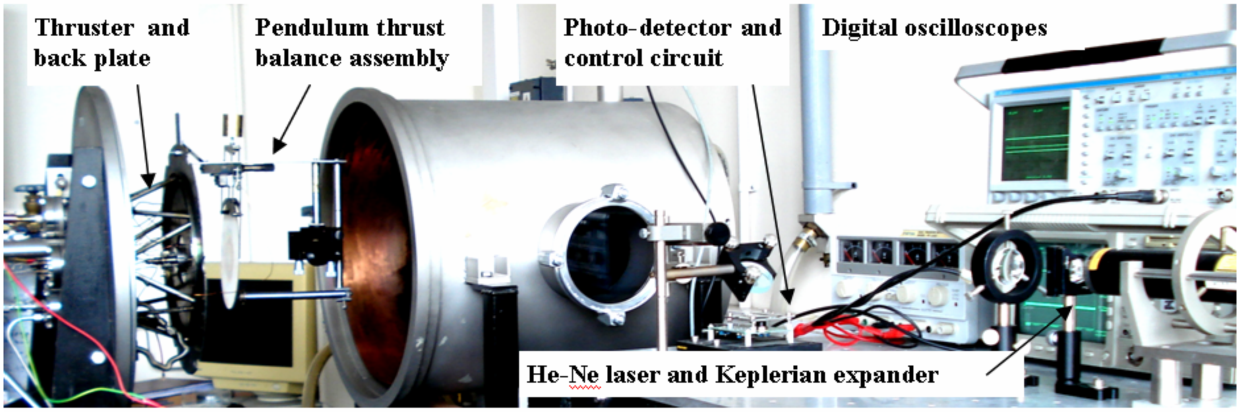

Figure 9 Experimental setup

The strike voltage is supplied by a pair of Farnell Hivolt PM1/DCP photo-multiplier supplies connected in parallel and powered by a pair of Farnell 16RA24012 linear 24V power supplies. Once the discharge is initiated, steady state power is provided by a Glassman LV80-37 DC power supply. This is a 3kWswitch mode supply with load regulation of +/-0.1% and an output ripple of 10mV RMS over the frequency range 20Hz-20MHz. Plasma noise and instabilities in the discharge are monitored with a Gould 1600 digital oscilloscope connected across the anode power supply. Anode voltage current characteristics are monitored via the supply digital meters, limiting the resolution of the readings to +/- 0.1A and +/- 0.001V, while strike voltage was monitored by a digital multi-meter with a resolution of +/-0.001V.

Optical Thrust Measurement System

Optical setup consists of a Miles Grilot He-Ne (543.5nm) laser passed through a Keplerian beam expander and directed through the chamber onto a mirror, rigidly connected to a molybdenum pendulum target shown in Figure 10. The optics system guides the reflected beam out of the chamber and onto a Hamamatsu 4.7 x 4.7mm two-dimensional tetra-lateral photo-sensitive-detector (resolution of 600nm) at a path length of 0.86m. The detector is coupled with a C4674 signal processing circuit (output +/- 2.5V at 1V/mm on each axis) is designed to provide two-dimensional position data on the incident light spot independent of the light intensity and is powered by a 30V Instec dual-tracking power supply (ripple less than 3mV). The output from the signal processing circuit is displayed on a Tektronix TDS 410A 2-channel digital oscilloscope (resolution +/- 0.001V). A pivoting mechanism allows the target to be positioned both perpendicular to the thrust vector and through a full 90˚ sweep of angles, while also allowing the pendulum to be electrically floated, grounded or biased. The pendulum thrust balance, shown in Figures 9, is mounted on a beam fixed to the UK-25 ion thruster back plate and is positioned with the cathode on axis with the centre of the target.

Unwanted oscillations in the system are passively damped by magnetic induction of a weak magnet placed close behind the Molybdenum target, electrically dissipating energy in the system. The optical detection setup of a green He-Ne laser mounted externally, two convex lenses forming a Keplerian beam expander and four mirrors.

RESULTS AND DISCUSSION

Cold Gas and Resistojet Thrust Measurement

The hollow cathodes can be operated in a cold gas and resistojet mode (with the cathode heater only operating) in addition to the discharge mode. The system therefore allows for 2-levels of partial redundancy if the discharge is not able to ignite. Tests were conducted with argon and xenon for the T6 cathode to characterize possible performance in these two modes and give some indication of the degree of elastic or non-elastic collisions with the target. Figures 10 and 11 show the thrust and specific impulse obtained when operating in a cold gas and resistojet mode. During the heated mode, the cathode was operated at 50W heater power with the.

The T6 thruster shows relatively poor specific impulse with xenon as expected; improving with the lighter molecular gas. Error bars are indicative of thrust measurement inaccuracies due to external excitations of the thrust balance, primarily from the roughing pump. Thrust measurements were made with good repeatability down to approximately 0.08mN, after which it became difficult to resolve thrust measurements with the sensitivity of the current balance setup.

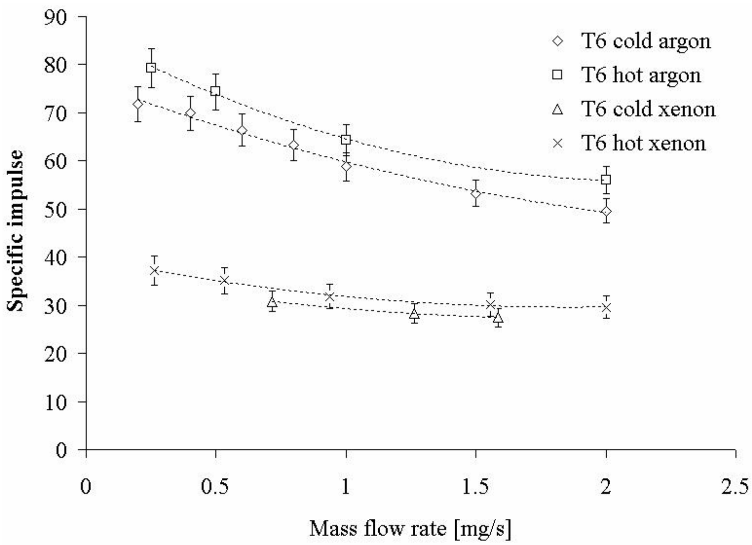

Figure 10 Specific impulse obtained operating the T6 cathode (argon and xenon) in a cold gas and resistojet mode (using only the heater)

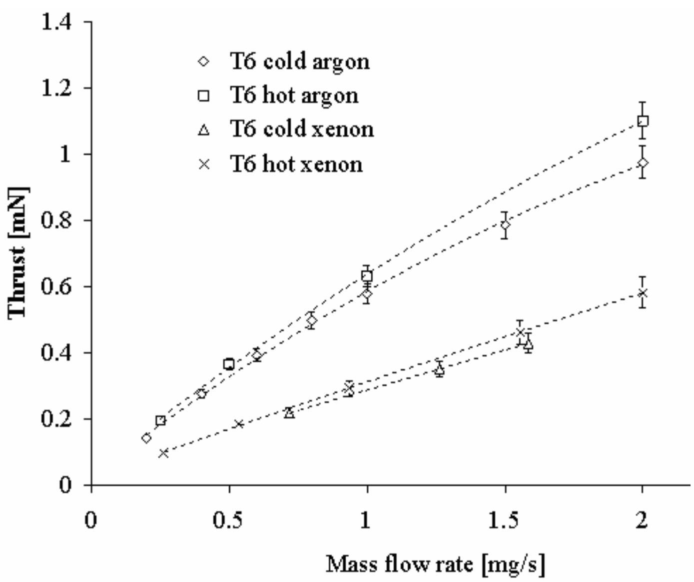

Figure 11 Thrust obtained from operating T6 cathode (argon and xenon) in a cold gas and resistojet mode

The orifice of the T6 cathode does act as a simple flat plate orifice since a higher internal pressure is maintained and thus a greater thrust produced by the adiabatic expansion. During the heated mode, higher internal pressure also allows a greater residence time for the propellant inside the cathode, giving a small improving heat transfer from the cathode walls by conduction. This increase in heat transfer raises the chamber pressure further. The increase in performance is fairly poor when considering the respective heater input power owing to the low chamber pressure and poor heat conduction from the cathode surface. The T6 cathode achieved a maximum Isp of 72 seconds with argon and 77-seconds with xenon at 0.14mN and 0.095mN respectively obtained in resistojet mode. The loss of performance at higher mass flow rates is likely due to greater interaction between the expansion plume and the anode orifice edge and face.

Initiation of the Discharge

One factor important for operation in a discharge mode is the reaction time of the system. Since hollow cathodes require heating prior to ignition, this has to be taking into account when considering power budgets and the sequencing of thruster firings. Prior to ignition the T6 heater was operated at 2.5A +/- 0.1A respectively for approximately 20 minutes to begin thermionic emission from the dispenser. Since power supplies were current limited, the heater voltage drop determined the input power. Figure 12 shows the results of 20 ignition characterization cases for the T6 cathodes, along with a typical heater power profile.

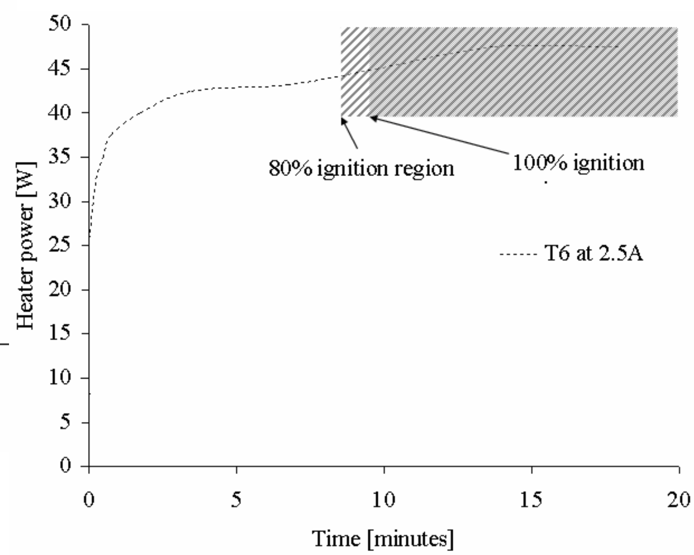

Figure 12 Heater input power over the pre-ignition heating period for the T6 cathode showing the times at which 80% and 100% of the test cases gained ignition

In the case of the T6 cathode, the heater is primarily radiative rather than conductive; therefore the voltage increases very rapidly at the start of the cycle. As the assembly heats up there is only a small increase in heater power due to the limited conductivity. The cathode ignited readily at around 7.5 minutes, while all ignitions had occurred by approximately 9.5 minutes.

Strike Voltage

Although a strike voltage was available to initiate electrical breakdown the anode voltage (set at 70V) was always sufficient to initiate all discharges. In application as a thruster especially on small satellites the breakdown voltage is important due to limited power electronics resources, generally consisting of an unregulated 28V bus and regulated 5V bus. In an attempt to quantify the maximum operating voltage an investigation was made recording the breakdown potential for 20 consecutive start-ups. In the case of the T6 variant cathode, the anode cathode separation (0.5mm) considerably reduced the startup voltage. It was found that initiation was always possible so long as the voltage limit on the power supply was set higher than that of the cathode during operation at the respective mass flow rate, particularly with xenon. In this case the start-up voltage operating with 0.5mgs^{-1} was consistently less than 12V.

Current Voltage Characteristics

Current voltage characteristics were obtained for operation of the T6 over the flow range 0.05-mgs^{-1} to 1-mgs^{-1} and at 10A, 20A, 25A and 30A with argon and 20A with xenon.

Plasma contact area was considered in the modified T6 cathode design primarily based on Equation (9), and maximizing the available contact area between the emitted plasma and the anode without significantly impeding the flow. This maximized thrust at reasonable discharge voltages while maintaining diffuse arc attachment. The very low operating voltages shown in Figure 14 are testament to this relationship. The discharge voltage in the T6 case only began to increase significantly (>15V) below 0.25mgs^{-1} for even the highest discharge currents (30A) with the lowest possible flow rate being 0.045mgs^{-1} at 28V with argon and 0.040mgs^{-1} at 42V with xenon. Above this flow rate there was little discernable difference in discharge voltage at all current conditions. Such low flow rates can not be obtained without suitable anode design and to the authors knowledge these are the lowest flow rates that a T6 cathode has ever been operated at while drawing such high discharge currents.

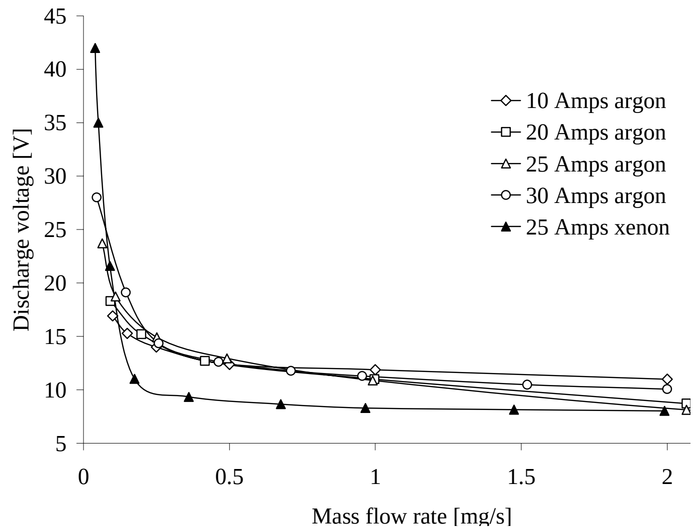

Figure 13 Current-voltage characteristics for the modified T6 cathode with argon and xenon

Operation with xenon gave consistently lower discharge voltages (testament to the lower primary ionization energy) and showed arguably the most impressive current voltage characteristics with the cathode delivering 25Amps at only 0.15mgs^{-1} and 12V discharge voltage. Operation at higher mass flow rates gave reduction down to 8V. It should also be noted that there was also no transition to unstable modes of operation at very low mass flow rate in the modified T6 design. Discharge voltage is always stable and down to a critical point of mass flow rate when the cathode extinguishes, the reduction in back pressure encourages an increase in mass flow through the orifice and the cathode then enters into a pulsed mode of operation, continuously igniting and extinguishing until after a short time, the assembly temperature drops and the ignitions do not continue. The increase in discharge voltage at low flow rate suggest a similar phenomenon to that found in MPD thrusters termed the ‘critical current’ and is close to the full ionization current, at which nearly all the propellant is ionized and exhausted at the critical Alfven velocity.[38] [39]

T6 Discharge Thrust Measurement

It should first be noted that to ensure the target was not being influenced by the plasma in which it is immersed, the target was biased +/- 30V and also directly grounded during high and low power operation. The thrust measurement system showed no sign of plasma interaction with the thrust balance affecting the thrust measurements.

Operation of the cathode at high and low power levels is shown in Figures 14 and 15 respectively.

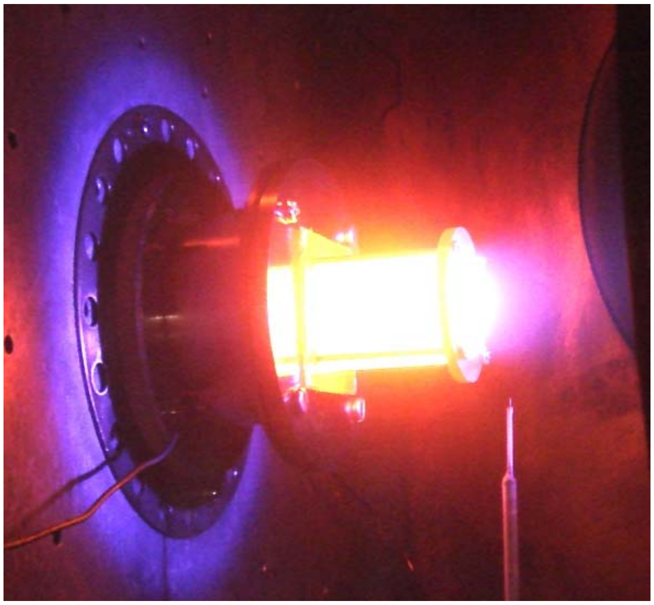

Figure 14 T6 cathode operating stably at 840W (30Amps) on argon at 0.045mgs-1, 28.0V discharge voltage

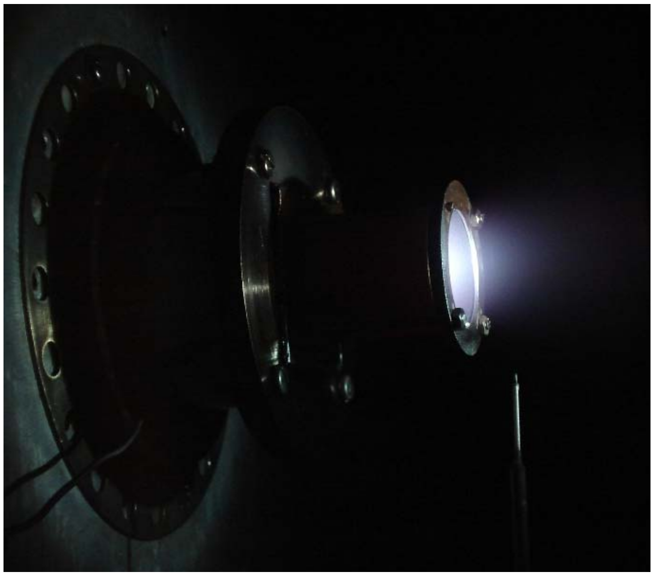

Figure 15 T6 operating on xenon at 200W (25Amps) 0.5 mgs^{-1} at 8.01V discharge voltage

Figure 16 shows that ultimately high specific impulse is dependant on discharge current since higher discharge currents are able to sustain operation at lower mass flow rates and higher powers. Operation with xenon also gives high specific impulse although only at the lowest flow rates. This is testament to the lower primary ionization energy of xenon, which enabled the cathode to operate at the lowest flow rate of 0.04mgs^{-1}. The T6 cathode shows relatively little improvement in specific impulse at higher currents indicating that resistive dissipation plays only a much small role in thrust production, which is reasonable due to the large orifice with current densities of 38A.mm^{-2}.

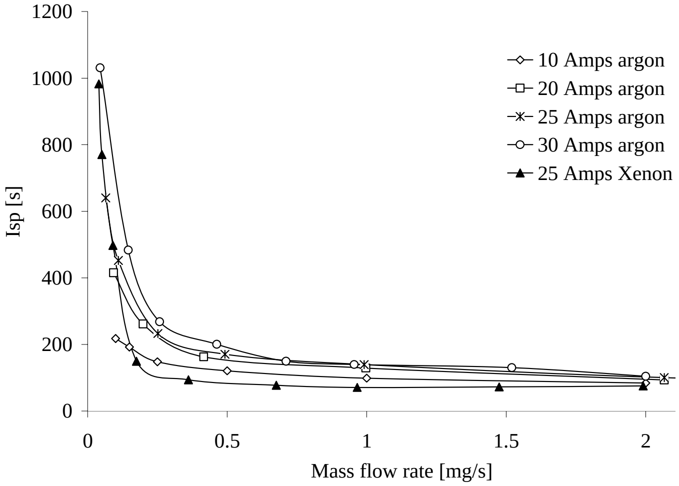

Figure 16 Specific impulse reached with the modified T6 hollow cathode at various current conditions and mass flow rates

Figure 17 shows two distinct gradients in the relationship between specific power and specific impulse. For operation with argon, specific impulse is almost identical for low specific powers, however approaching 5000J.mg^{-1} there is a change in gradient.

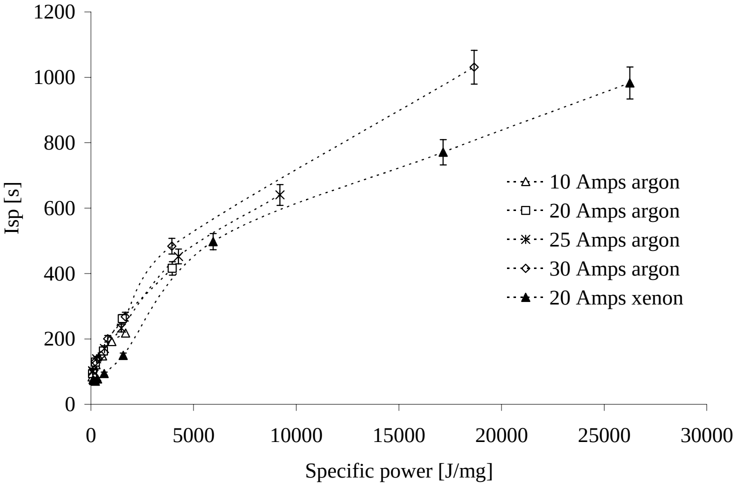

Figure 17 Relationship between specific impulse and specific power for the T6 at various current levels with xenon and argon

It is postulated that this change in gradient is also a change in dominant thrust mechanism, with electromagnetic acceleration becoming the dominant accelerating mechanism, since flow rates above 5000J.mg^{-1} are very low and would contribute an increasingly small degree of electrothermal thrust. This theory is strengthened when considering thrust level with respect to mass flow rate as in Figure 18.

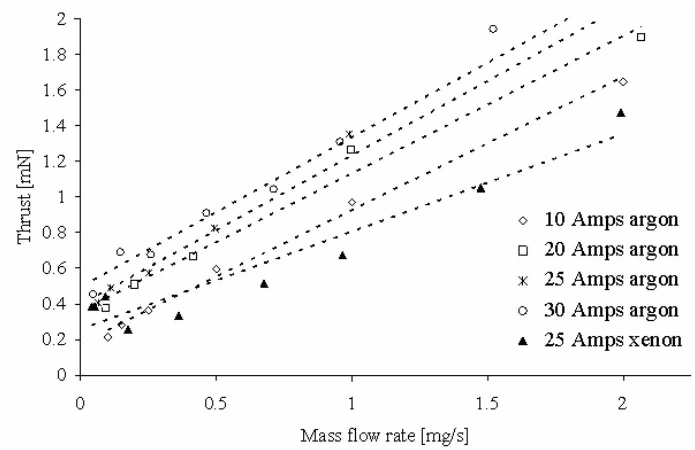

Figure 18 T6 thrust level with respect to mass flow rate at various current conditions with xenon and argon

It is clear that when extrapolating thrust level back to zero mass flow a remnant thrust production mechanism exists which is dependant on discharge current. The nature of this mechanism is made clear when overlaying the theoretical specific impulse obtainable by electromagnetic blowing force with the results obtained from the T6 cathode, shown in Figure 19.

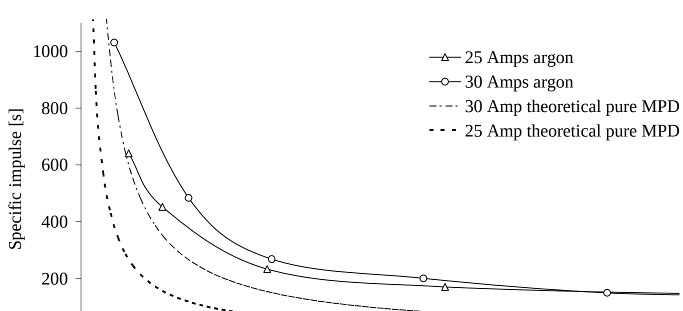

Figure 19 Experimental and theoretical specific impulse obtained from operation at 25 and 30 Amps with the modified T6 cathode with argon

The result shows a high likelihood that the increased specific impulse found at low and minimum mass flow rate is almost entirely due to MPD forces acting on the plasma. If the theoretical values are subtracted from those found in experiment consistent values of specific impulse between 200 and 300 seconds remain, explicable by the additional thermal thrust production mechanism. Since large discharge currents are required to produce a relatively small blowing force, thrust to power ratios are far below 1% in all but the 30A case for high specific impulse.

VI. Conclusion

The exact thrust mechanisms of the T6 hollow cathode have been debated for some time. Our results indicate that for high specific impulse the hollow cathode operates as a low power MPD thruster. Due to the relatively low currents, electron convective and radiative losses dominate performance and thus give poor thrust efficiencies. Operation at elevated currents is likely to significantly improve performance and thrust efficiency; although this will be well beyond the rated current capacity for the T6 cathode. Subtracting the thrust production by electromagnetic acceleration would indicate that while electrothermal acceleration does play a role in T6 thrust production, it does not increase significantly as mass flow is decreased. This suggests that either electron temperature does not increase significantly at lower flow rates or that the energy equipartition between electrons-ions and electron-neutrals remains too low for any substantial increase in heat transfer.

The low voltages obtained in the modified T6 design highlight the importance of plasma anode interaction and cathode and keeper design. Previously keeper design has been considered relatively insignificant; however as has been shown optimized keeper design is imperative for hollow cathode thrusters, but also for neutralizers for Hall thrusters, ion engines and plasma contactors for minimization of discharge voltage and propellant loss. It should also be noted that the artificial backpressure becomes important at low mass flow rates are decreased as a means to maintain higher internal pressures. The T6 design also highlights the effect of anode cathode spacing on ignition voltage and potential for further optimization. The T6 in its current form could operate from a regulated 28V bus on large and small spacecraft without the need for high strike voltages.

This work suggests that hollow cathode thruster research can be split into two domains; low current, low power hollow cathodes which work on a resistive plasma heating mechanisms with small internal geometries, and higher current, hollow cathodes which benefit from MPD acceleration mechanisms. Indeed multi-channel hollow cathodes have been proposed and built for MPD thrusters for some time. If the hollow thruster is to have a place in the family of MPD accelerators, it may as a very low power thruster <2kW (owing to the very low discharge voltages) with very little power conditioning. Thrust efficiencies are unlikely to improve significantly since this will scale quadratically with discharge current and will quickly enter much higher power regimes of operation.

At this time no investigation has been possible into the effect of elastic and non-elastic collisions with the target. This effect may be significant due to the planar geometry of the target. The effect is visible in operation of the cold gas thruster. The theoretical specific impulse for this type of operation should be around 50s with argon, the apparent specific impulse is around 80s. It should therefore be noted that this overestimation of thrust and thus specific impulse will also be consistent in the results for operation in a discharge mode at this preliminary stage. Future work will therefore be aimed at designing a pendulum target which is able to limit the effect of elastic collisions by controlling particle paths.

ACKNOWLEDGEMENTS

The author would like to dedicate this work to the late David Fearn; a master of his field and a gentleman whom without, this work would not be possible. His continued dedication to his field over the last 50-years has brought about revolutions in electric propulsion, and to those who knew him he was truly one of the greats. His knowledge, humor and company will be sorely missed.

REFERENCES

[1] Gray, H L, "*Development of ion propulsion systems*", *GEC Rev,* 12, 3, 154-168, 1997.

[2] Wallace, N C and Feam, D G, "The *design and performance of the T6 ion thruster*", AIAA Paper 98-3342, 1998.

[3] Fearn, D, Singfield, A, Wallace, N, Gab-, S and Harris, P, "*The operation of ion thruster hollow cathodes using rare gas propellants*", AIAA Paper 90-2584, 1990.

[4] Latham, P M, Martin, A R and Bond, A, "*Design, manufacture and performance of the UK-25 engineering model thruster*", AIAA Paper 90-2541, 1990.

[5] Harris, P T and Gair, S, "*A review of the cathode construction for the RAE 10/25 mN thruster*", IEPC Paper 88-078, 1988.

[6] Philip, C M and Fearn, D G, "*Recent hollow cathode investigations at the Royal Aircraft Establishment*", AIAA paper 73-1137, (1973); AIAA J, 12, 10, 1319-25, 1974.

[7] Fearn, D G, "*The operation of hollow cathodes under conditions suitable for ion beam neutralization*", Proc Conf on Electric Propulsion of Space Vehicles, Culham Laboratory, UK, (April 1973). Inst of Electrical Engineers Conference Publication 100, pp 146-150, 1973.

[8] S. Pottinger, P. Gessini, D. Webb, R. Intini Marques and S. B. Gabriel, "*Electric Propulsion Research at the University of Southampton*", Journal of the British Interplanetary Society, Vol. 59, No. 5, May 2006.

[9] P. Gessini, S. B. Gabriel and D. G. Fearn, "*Thrust Characterization of a T6 Hollow Cathode*", IEPC Paper 05-257, 29th International Electric Propulsion Conference, Princeton, NJ, October-November 2005.

[10] P. Gessini, S. B. Gabriel and D. G. Fearn, "*The T6 Hollow Cathode as a Microthruster*", AIAA Paper 2005-4078, 41st AIAA/ASME/SAE/ASEE Joint Propulsion Conference & Exhibit, Tucson, AZ, July 2005.

[11] Rayman, Marc D. and David H. Lehman, "NASA's First New Millennium Deep-Space Technology Validation Flight," Second IAA International Conference on Low-Cost Planetary Missions, Laurel, MD, April 16-19, 1996, IAAL-0502.

[12] P. Bodin, S. Berge, M. Bjork, A. Edfors, J. Kugelberg and P. Rathsman "*The SMART-1 Attitude and Orbit Control System: Flight Results from the First Mission Phase*", AIAA-2004-5244 AIAA Guidance, Navigation, and Control Conference and Exhibit, Providence, Rhode Island, Aug. 16-19, 2004

[13] H. Kuninaka, Y. Shimizu, T. Yamada, I. Funaki and K. Nishiyama,,"*Flight Report During Two Years on HAYABUSA Explorer Propelled by Microwave Discharge Ion Engines"*, AIAA-2005-3673, 41st AIAA/ASME/SAE/ASEE Joint Propulsion Conference and Exhibit, Tucson, Arizona, July 10-13, 2005

[14] Rayman, M. D., Fraschettia, T. C., Raymonda, C. A., Russell C. T, "Preparing for the Dawn Mission so Vesta and Ceres", IAC-05-A3.5.B.011, 56th International Astronautical Congress, 17 - 21 October 2005, Fukuoka, Japan,

[15] Moerel, J., Marée, T., Bombelli, V., Simon D.,

"*Economic Benefits of the Use of Non-Toxic Mono-Propellants for Spacecraft Applications*" , AIAA-2003-4783 39th AIAA/ASME/SAE/ASEE Joint Propulsion Conference and Exhibit, Huntsville, Alabama, July 20-23, 2003

[16] Jankovsky, R. S., Sankovic, J. M., Oleson, S., "*Performance of a FAKEL K10K resistojet*", AIAA-1997-3059 AIAA/ASME/SAE/ASEE Joint Propulsion Conference and Exhibit, 33rd, Seattle, WA, July 6-9, 1997

[17] Coxhill, I., Gibbon, D.,"*A Xenon Resistojet Propulsion System for Microsatellites*", AIAA-2005-4260 41st AIAA/ASME/SAE/ASEE Joint Propulsion Conference and Exhibit, Tucson, Arizona, July 10-13, 2005

[18] Coletti, M., Grubisic, A. Wallace, N., Wells, N., "*European Student Moon Orbiter Solar Electric Propulsion Subsystem Architecture – An All–Electric Spacecraft*" IEPC-2007-111 30th International Electric Propulsion Conference, Florence, Italy September 17-20, 2007 M.

[19] Walker, R., "*The SIMONE Mission: low-cost Exploration of the Diverse NEO Population via Rendezvous with Microsatellites*", IAC-03-Q.5.05 54th International Astronautical Congress of the International Astronautical Federation, the International Academy of Astronautics, and the International Institute of Space Law, Bremen, , Sep. 29-3, 2003

[20] Inter-Agency Space Debris Coordination Committee, Space Debris Mitigation Guidelines, IADC 02-01 (2002)

[21] Baker, A. M., Da-Silva-Curiel A, Schaffner, J., Sweeting, M. "Advanced Low Cost Propulsion Concepts for Small Satellites Beyond LEO", IAC Paper No. 04-IAF-S.1.08 (2004).

[22] Manzella, D. H.; Curran, F. M.; and Zube, D. M., "Preliminary Plume Characteristics of an Arcjet Thruster," AIAA Paper No. 90- 2645 (1990).

[23] Mueller J., "*Thruster Options for Microspacecraft" from "Micropropulsion for Small Spacecraft*" Volume 187 Progress in Astronautics and Aeronautics.

[24] Cronin, J.L., "*Modern Dispenser Cathodes*" IEEE Proc. 128, 19–32 (1981).

[25] Martin, R. A., "*Atomic Excitation Processes in the Discharge of Rare Gas Ion-Engines*," J. Phys. BLAtom. Molec. Phys., Vol. 7, No. 10 (1974).

[26] Sarver-Verhey, T. R., "*28,000 Hour Xenon Hollow Cathode Life Test Results,*" IEPC Paper No. 97-168 (1997).

[27] Rawlin, V. K., "*A 13,000 Hour Test of a Mercury Hollow Cathode*," NASA TM X-2785 (1973).

[28] Sarver-Verhey, T.R., "*Extended Test of a Xenon Hollow Cathode for a Space Plasma Contactor,*"NASA CR–195402 (1994).

[29] Polk J.E., Grubisic A. N., Goebel D., "*Emitter Temperature Distributions in the NSTAR Discharge Hollow Cathode*" AIAA-2005-4398, 41st AIAA/ASME/SAE/ASEE Joint Propulsion Conference, Tucson, AZ, 2005

[30] Grubisic A.N., "*Temperature Characterization and Optimization of an NSTAR Discharge Cathode for the Deep Space-1 Gridded Ion-Engine*" Masters Thesis, International Space University, Strasbourg, France 2005

[31] Rehn, L. and Kaufman, H.R., "*Correlation of Inert Gas Hollow Cathode Performance,*" AIAA Paper No. 78-707 (1978).

[32] Sahli, A., Turchi, P.J., "*Low Power Plasma Thruster Based on a Hollow Cathode Discharge*", AIAA Paper No. 94-3126 (1994).

[33] Williams, G., Smith, T., Domonkos, M., Shand, K., and Gallimore, A., "*Laser Induced Fluorescence Characterization of Ions Emitted from a Hollow Cathode,*" AIAA Paper No. 99-2862 *(*1999).

[34] Domonkos, M. T., Gallimore, A. D., and Patterson, M. J., "*An Evaluation of Hollow Cathode Scaling to Very Low-power and Flow Rate*," IEPC Paper No. 97-189 *(*1997).

[35] Katz, I. and Patterson, M. J., "*Optimizing Plasma Contactors for Electrodynamic Tether Missions,*" Tether Technology Interchange, Huntsville, AL, Sept. 1997.

[36] Mikellides I., Katz ., Goebel D. M., and Polk J. E., , "*Theoretical Model of a Hollow Cathode Plasma for the Assessment of Insert and Keeper Lifetimes*", AIAA Paper No. 2005-4234 (2005).

[37] C. H. Edwards "*Discharge Characteristics and Instabilities in the UK-25 Ion Thruster Operating on Inert Gas Propellants*" PhD. Thesis, University of Southampton, 1997.

[38] R. H. Frisbee, N. J. Hoffman, "*Electric Propulsion Options for Mars Cargo Missions*"., AIAA paper, 32nd Joint Propulsion Conf. (JPC), Lake Buena Vista (FL), July 1996.

[39] M. Andrenucci et al., "*Scale and Geometric Effects on the Performance of MPD Thrusters*", AIAA 92-3159, 28th JPC, Nashville, TN, July 1992.